Synthesis, Microstructure and Mechanical Properties of Mg. 5Zn. 0.3Ca/nHA Nanocomposites

N. Aboudzadeh[1], Ch. Dehghanian[1, *] and M. A. Shokrgozar[2]

* *cdehghan@ut.ac.ir*

Received: June 2017 Accepted: October 2017

[1] University of Tehran, College of Engineering, School of Metallurgy and Materials Engineering, Tehran, Iran.
[2] National Cell Bank of Iran, Pasteur Institute of Iran, Tehran, Iran.
DOI: 10.22068/ijmse.14.4.58

Abstract: *Recently, magnesium and its alloys have attracted great attention for use as biomaterial due to their good mechanical properties and biodegradability in the bio environment. In the present work, nanocomposites of Mg. 5Zn. 0.3Ca/ nHA were prepared using a powder metallurgy method. The powder of Mg, Zn and Ca were firstly blended, then four different mixtures of powders were prepared by adding nHA in different percentages of 0, 1, 2.5 and 5 %wt. Each mixture of powder separately was fast milled, pressed, and sintered. Then, the microstructure and mechanical properties of the fabricated nanocomposites were investigated. The XRD profile for nanocomposites showed that the intermetallic phases of $MgZn_2$, $MgZn_{5.31}$ and Mg_2Ca were created after sintering and the SEM micrographs showed that the grain size of nanocomposite reduced by adding the nHA. The nano composite with 1wt. % nHA increased the density of Mg alloy from 1.73 g/cm^3 to 1. 75 g/cm^3 by filling the pores at the grain boundaries. The compressive strength of Mg alloy increased from 295MPa to 322, 329 and 318MPa by addition of 1, 2.5 and 5wt. % nHA, respectively.*

Keywords: *Powder Metallurgy, Metal Compositing, Mechanical Property, Mg.*

1. INTRODUCTION

Magnesium is a metallic biomaterial with bioresorbable property (1), which has been chosen as a candidate for bone tissue engineering (2). Good biocompatibilities and mechanical properties of magnesium alloys as temporary biomaterials are the main advantages for that(3). Most metallic implants are too stiff (young's modulus 100-200Gpa) but Mg has an elastic modulus (young's modulus 40-45Gpa) close to natural bone (young's modulus 10-30Gpa). therefore, stress shielding which is a challenge for metallic implant will be reduced in bone tissue near magnesium implants(4, 5). High speed degradation of Mg is the main limitation for its implementation as an orthopedic biomaterial. Destruction of Mg implant occurs prior to a formation of stable tissue around it; therefore, prevention of Mg corrosion is significant(6).

Alloying with a few elements such as Zn, Mn, Zr, Ca and a very small concentration of low toxicity rare earth (RE) elements (7) is one of the most effective methods to improve the corrosion resistance of magnesium. Many researchers have focused especially on the Mg-Ca(2), Mg-Zn (8) and Mg-Zn-Ca (8, 9) alloys in order to introduce biodegradable bone implants. Ca and Zn have a considerable effect on improving both corrosion resistance and mechanical properties of Mg (10).

Another approach which is propounded for Mg alloy to meet the requirements for bone tissue engineering is to composite Mg alloy with biocompatible and bioresorbable reinforcement (11). Biodegradable and bioactive particles as reinforcement improve both corrosion resistance and mechanical properties of Mg alloy. Bioactive reinforcements increase growth of osteoblast cells and decrease reparation time, which is valuable for Mg implants. Calcium phosphates like hydroxyapatite and tri-calcium phosphate as a biomaterial with excellent biocompatibility, biodegradability, osteoconductivity and non-toxic properties could be an appropriate reinforcement for Mg alloys (11).

Different methods are being used for compositing Mg with calcium phosphate

reinforcement, such as casting (12), high frequency induction heat sintering (HFIHS)(11), friction stir process (FSP) (13), equal channel angular extrusion (ECAE) (14) and powder metallurgy(15). Powder metallurgy (PM) technique prepares nanocomposites with homogeneity in the reinforcement distribution which is challenging to be achieved by the conventional casting method(16). In this paper both alloying and compositing of Mg were done by powder metallurgy process to make Mg suitable for bone tissue repairing. The aim of the present study is to fabricate Mg-5Zn-0.3Ca/nHA nanocomposites with different percentages of nHA and to investigate its mechanical properties.

2. EXPERIMENTAL

2. 1. Material Preparation

Powders of magnesium (Mg, 97% ≤ purity), zinc (Zn, 95% ≤ purity) and calcium (Ca, 98.5% ≤ purity) purchased from Merck (Darmstadt, Germany) and nHA powders were synthesized in our laboratory were used as starting materials. The nHA powders were synthesized by reaction of $CaCl_2$ with Di ammonium hydrogen phosphate (DAHP) as described in reference(17). The $CaCl_2$ solution was added dropwise to the $(NH_4)_2HPO_4$ solution at room temperature until a white precipitate appeared. The Ca/P ratio was kept constant at 1.67 and the reaction pH was maintained above 10-11 throughout the reaction period. The white precipitate was then aged for 17 h and washed with distilled water three times to remove the residual salts and lower the pH.

The proper percentages of pure Mg, Zn, Ca and nHA powders in composite sample were firstly blended then fast milled for 6 min and then pressed by a uniaxial press at 400Mpa pressure in two sizes of 10 Φ×5 mm^2 and 10 Φ×15 mm^2 and heated at a rate of 10°C/min to reach 550°C in a tube furnace under the Argon atmosphere for 2 hours. Mg-5Zn-0.3Ca alloy and Mg-5Zn-0.3Ca/X nHA (X= 1, 2.5 and 5 wt. %) nanocomposites were classified as MZC, MZC-1nHA, MZC-2.5nHA and MZC-5nHA, respectively.

2. 2. Metallurgical and Mechanical Testing

Thermal behavior of four different mixtures of powders were evaluated by differential thermal analyses (STA503, Germany) to select the sintering temperature. Differential thermal analyses (DTA) for powders was done at a heating rate of 10°C/min from ambient temperature to 700 °C under Argon atmosphere.

Micro structure and elemental analyses of nanocomposite samples were done using scanning electron microscopy (SEM: TSCAN-VEGA, China) and energy dispersive X-ray spectroscopy (EDS: TSCAN-VEGA, China), respectively. X-ray diffraction (XRD: JDX-8030, Jeol, Japan) with a Cu-Ka source was used to obtain the diffraction patterns for samples. The identification of all reflections was accomplished using the X'Pert software.

The densities of specimens (ρ) were measured and calculated by Archimedes equation as follow:

$$\rho=\rho_{liq}(M_{dry}/M_{dry}-M_{submerged}) \quad (1)$$

where ρliq is the density of oil, M_{dry} is dry weight and $M_{submerged}$ is submerged weight of the specimen. The theoretical density of specimens (ρ_{th}) was also calculated by Eq. (2):

$$\rho_{th}=(w_1+w_2)/((w_1/\rho_1)+(w_2/\rho_2)) \quad (2)$$

where (w_1, w_2) and (ρ_1, ρ_2) are weight fractions and theoretical densities of each constituent, respectively.

A compressive test was carried out according to ASTM E9-09 standard (18) for compression testing of metallic materials at room temperature by SANTAM (STM-20) testing machine on specimens with a diameter of 10 mm and a thickness of 15 mm at room temperature with a rate of 1 $mm.s^{-1}$.

3. RESULTS AND DISCUSSION

3. 1. DTA–TGA Analysis

The DTA for MZC, MZC-1nHA, MZC-2.5nHA and MZC-5nHA samples indicated an endothermic peak around 650ºC and an

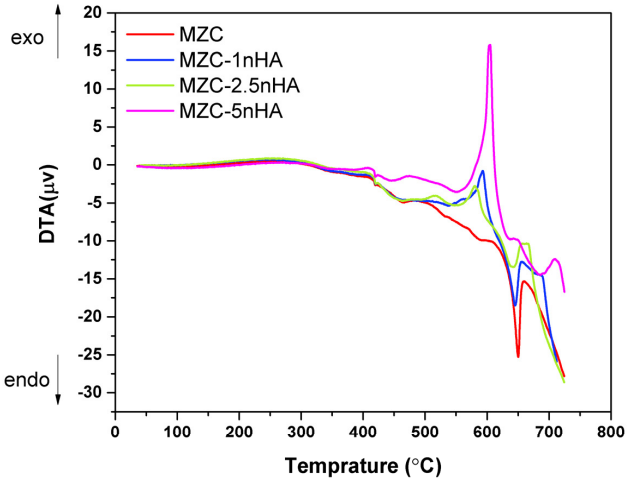

Fig. 1. DTA plots for MZC, MZC-1nHA, MZC-2.5nHA and MZC-5nHA.

exothermic peak around 600ºC (Fig. 1). The endothermic peak should be related to melting point of powders and the exothermic peak may be related to interchanging of oxygen in nHA with metals(19) which was considered by studying XRD profile for sintered MZC-5nHA in section 1.2. According to DTA of powder mixtures, sintering temperature at 550ºC was selected for all sintering process of nanocomposites.

3. 2. Metallurgical and Mechanical Characterization

XRD profiles for MZC before and after sintering process are shown in Figs. 2a and 2b, respectively. The diffraction pattern for MZC before sintering process showed peaks of Mg and Zn. However, the low percentages of Ca caused its related peak not to appear. Comparing diffraction pattern of MZC before and after sintering process showed that Zn peaks were disappeared and instead intermetallic phases of $MgZn_2$, $MgZn_{5.31}$, and Mg_2Ca peaks emerged, so eutectic transformations happened at sintering process. The same intermetallic phase peaks were shown at XRD spectrum for sintered MZC-5nHA in Fig. 2c. So the presence of nHA in nanocomposites did not prevent from eutectic transformations at sintering process. It is

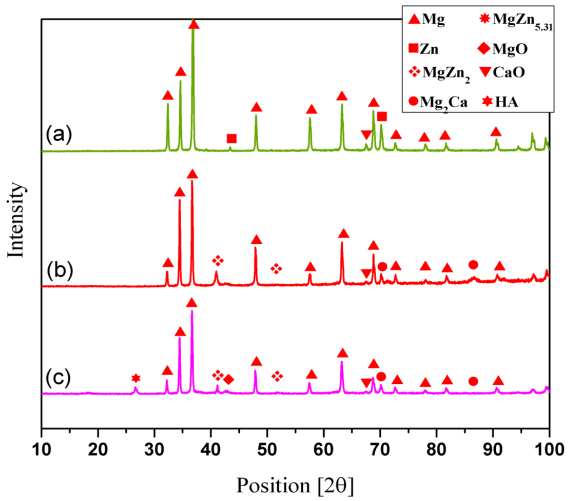

Fig. 2. XRD Pattern of the (a) MZC before sintering, (b) MZC and (c) MZC-5nHA after sintering.

important because these intermetallic phases increase mechanical and corrosion properties of alloys (8). XRD spectrum for MZC-5nHA also showed peaks of nHA and MgO. The MgO peak may be related to the reaction of Oxygen in HA with Mg at sintering temperature which showed an exothermic peak in DTA of MZC-5nHA.

Metallographic microstructures of samples after sintering process are shown in Fig. 3. The results indicated that the grain size of the nanocomposites was reduced by increasing nHA as a reinforcement. The same result was reported by Ahmadlhaniha et al. (20) for Mg/HA composite fabricated by FSP. In fact, the nano size particles were attached to the metal particle through mixing and prevented particle growth at sintering temperature(15), so the nano composites with higher percentages of nHA had smaller grain size.

Low magnification SEM micrographs of MZC is illustrated in Fig.4. Its elemental mapping revealed a relatively uniform distribution for Zn, Ca in the matrix, although some accumulations were seen in particle boundary. According to XRD and phase diagrams for Mg-Zn-Ca (21), these accumulations were outcome from production processes and eutectic reactions in particle boundaries at the sintering temperature. The EDS analysis for marked points was listed in Table 1.

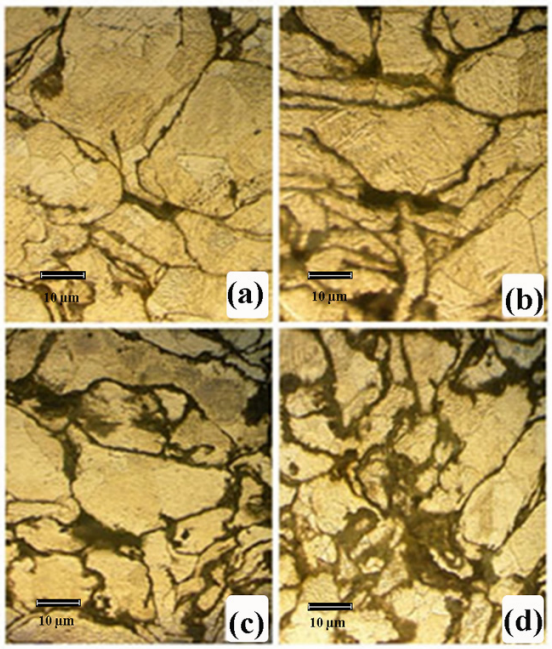

Fig. 3. Optical images of a) MZC, b) MZC-1nHA, c) MZC-2.5nHA, d) MZC-5nHA, sintered at 550 °C for 2h. (×500).

Low magnification SEM photomicrograph of MZC-5nHA gives a light on how nHA in particle boundaries refines the MZC structure and prevents the grain growth (see Fig. 5). Elemental mapping for MZC-5nHA surface shows that Zn

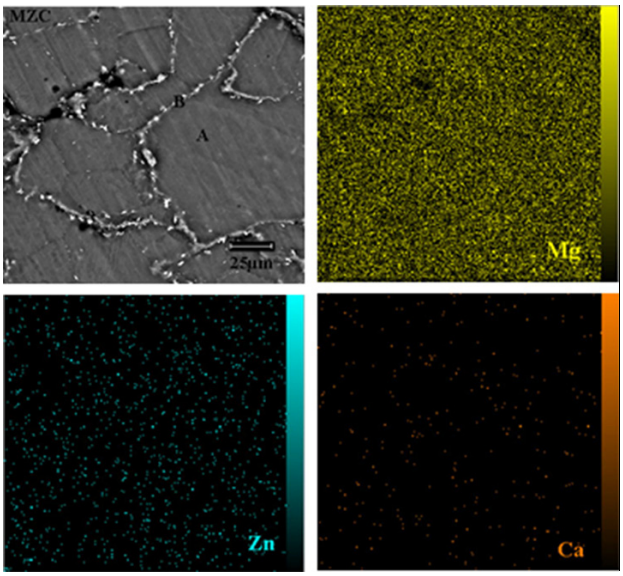

Fig. 4. Low magnification SEM micrographs of the MZC at ×3000 kv, and its elemental mapping.

Table 1. Energy dispersive X-ray Spectrometer analysis results of the MZC.

points	Mg content (wt. %)	Zn content (wt. %)	Ca content (wt. %)
A	95.46	4.54	-
B	91.29	8.44	0.27

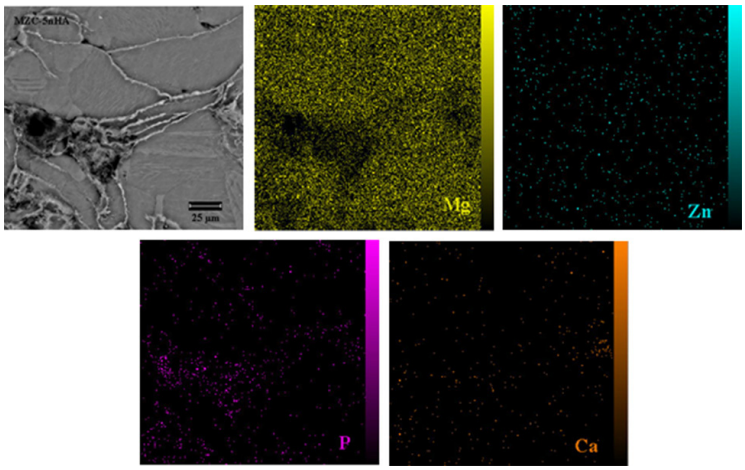

Fig. 5. Low magnification SEM micrographs of the MZC-5nHA at ×3000 kv, and its elemental mapping.

distribution is uniform but Ca and P mostly were accumulated at particle boundaries. These accumulations limited the grain growth at the sintering temperature.

Since the selected sintering temperature (550°C) is upper than the melting point of Zn(419.5°C) , it seems two mechanisms may be happen in sintering of nanocomposites, one liquid state and two solid state. The XRD profiles of nanocomposite showed that the liquid phase of Zn is not permanent and may be entered in eutectic transformation and established the intermetallic phase. So the liquid phase is transient and the solid state is the main sintering mechanism in nanocomposites.

Densities of samples which were determined by Archimedes equation are shown in Fig. 6 and summarized in Table 2. The results indicated that nearly dense Mg alloy and composites materials could be attained using the production procedure adopted in this study and there is low difference between theoretical and measured density. The results also revealed that density of MZC was improved from 1.73 g/cm^3 to 1.75 g/cm^3 by adding 1%wt nHA, but it was reduced to 1.72 g/cm^3 and 1.7 g/cm^3 by adding 2.5%wt and 5%wt nHA, respectively. Actually, the low percentage (1%wt) of nano powders may fill porosities in intersections of grains in matrix and enhance the density (22, 23). This was approved by SEM

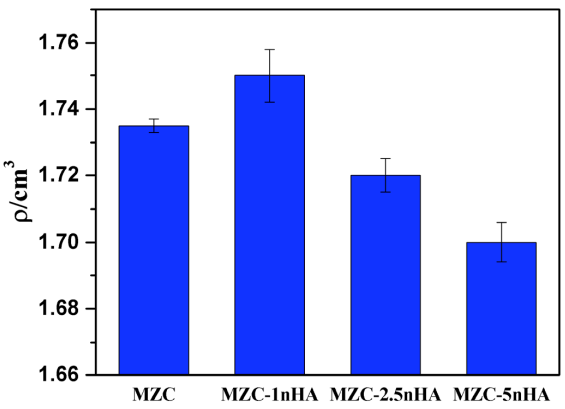

Fig. 6. Density of samples based on Archimedes law.

Table 2. Theoretical and Archimedes density of samples.

sample	ρ_{theory} (g/cm^3)	$\rho_{Archimedes}$ (g/cm^3)
MZC	1.8	1.73
MZC-1nHA	1.80	1.75
MZC-2.5nHA	1.819	1.72
MZC-5nHA	1.839	1.7

images of intersection of grains in MZC and MZC-1nHA after sintering in Figs. 7a and 7b. Actually, up to 1%wt. nHA, the powders fill porosities in intersections of matrix grains (24) and improve density of MZC, but with increasing nHA contents more than 1% wt., a decrease in density of nano composites was observed. The decline of density of nanocomposites was attributed to two reasons. First, increasing nHA contents more than 1% wt. created some agglomerations in grain boundaries which were observed for MZC-2.5nHA and MZC-5nHA in Figs. 7c and 7d. These agglomerations with pores inside and outside could reduce the density. Second, the sintering temperature of samples was selected to be lower than the melting point of metals at 550°C, but sintering temperature of pure nHA is about 1000°C (25, 26). Therefore, sintering temperature was considerably insufficient for achieving high densification in nHA particles and the density of nanocomposites decreased with an increase in nHA. However, the presence of porosity in implants with no significant influence on mechanical properties and corrosion rates may help tissue healing and formation of the bone tissue in the body(27).

The compressive stress–strain curve of MZC and nanocomposites are illustrated in Fig. 8. The yield strength (YS), ultimate compact strength (UCS) and elastic modulus of samples acquired from Fig. 8 are shown in Table 3. The elastic modulus of MZC was increased by the addition of nHA. Uniform distribution and good interfacial integrity of nHA (28) with its high elastic modulus can increase nanocomposites's modulus. The elastic modulus of nano composites is closer than those of other metal biomaterials like Ti alloys and stainless steel to the natural bone. This may cause lower stress

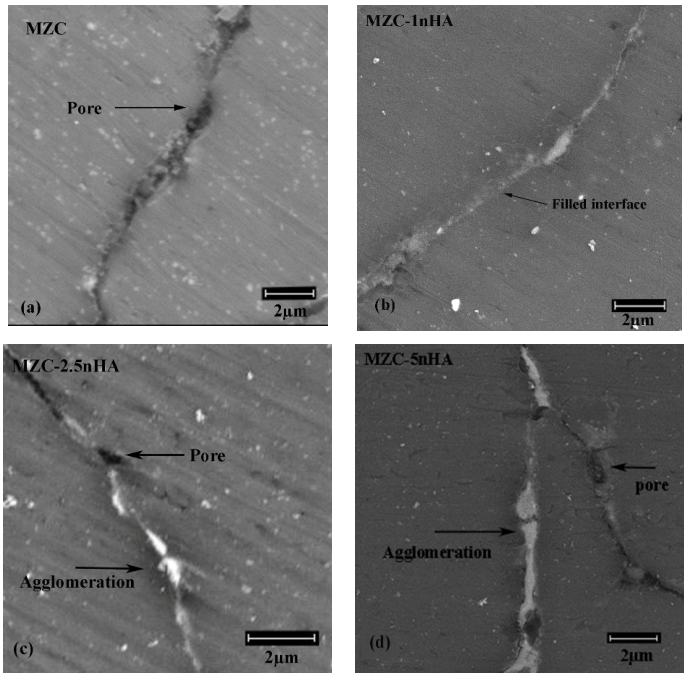

Fig. 7. SEM micrograph of intersection of matrix grains for a) MZC, b) MZC-1nHA, c) MZC-2.5nHA, d) MZC-5nHA after sintering.

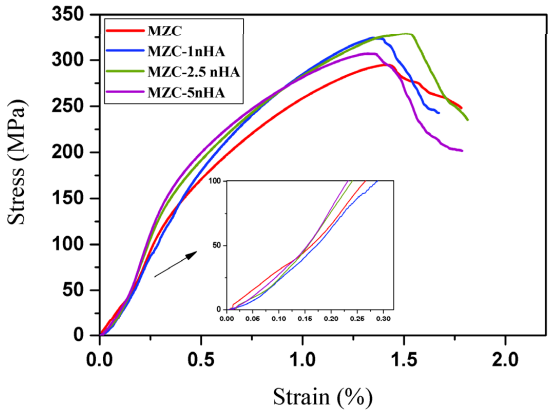

Fig. 8. Effect of nHA concentration on the typical stress–strain curve of nano composites.

shielding in bone.

The results also indicated that YS and UCS of MZC were improved by addition of nHA as reinforcement. The values of UCS for MZC were increased from 295MPa to 322, 329 and 318 MPa for MZC-1nHA, MZC-2.5 and MZC-5nHA respectively. MZC-2nHA nanocomposite shown the highest yield and ultimate compact strength.

In general, four possible strengthening mechanisms may be applied in Mg-5Zn-0.3Ca/nHA composite systems (29, 30), Orowan looping, strengthening due to grain refinement, mismatch in coefficient of thermal expansion (CTE) between nHA and matrix and load transfer.

The contributions of each strengthening mechanism to YS of the composite can be expressed as follows:

$$\sigma_{YS} = \sigma_{ym} + \Delta\sigma_{Orowan} + \Delta\sigma_{Hall-petch} + \Delta\sigma_{CTE} + \Delta\sigma_{LT} \quad (3)$$

where σ_{YS} is YS of the composites, σ_{ym} is the YS of the Mg alloy and $\Delta\sigma_{Orowan}$, $\Delta\sigma_{(Hall-petch)}$, $\Delta\sigma_{CTE}$, $\Delta\sigma_{LT}$ are the effect of four mentioned strengthening mechanisms (Orowan looping, strengthening due to grain refinement, mismatch in coefficient of thermal expansion (CTE) between nHA and matrix and load transfer , respectively) in YS of nanocomposite.

The nanoscale particles can strongly pin and hinder the movement of dislocation based on the Orowan mechanism (31, 32) and increased the YS as follow (29):

$$\Delta\sigma_{Orowan} = 0.8MGb\sqrt{\frac{2f_v}{\pi d^2}} \quad (4)$$

where M is the strengthening coefficient ~1.25 (33), G is the shear modulus of Mg matrix ~ 1.66 $\times 10^4$ MPa, b is the burger vector for Mg ~3.21×10^{-10} (29), d and f_v are the average diameter and volume fraction of nHA, respectively. Eq. (4) reveals that an increase in volume fraction of nHA cause an increase in $\Delta\sigma_{Orowan}$ of nanocomposite and in result increase the UCS of Mg-5Zn-0.3Ca/nHA composite.

The classical Hall-Petch relationship given in Eq. (5) (34) reveals that decreasing grain size will lead to an increase in YS.

Table 3. comparison of mechanical properties of sintered nanocomposites with other materials.

Material	YS (MPa)	UCS (MPa)	Modulus (Gpa)
MZC	63	295	38
MZC-1nHA	66	322	42
MAC-2.5 nHA	79	329	45
MAZ-5nHA	76	318	48
Natural bone		130–180	3-20
Ti alloy		758–1117	110–117
Stainless steel		480–834	70–230

$$\Delta\sigma_{Hall-petch} = k(\sqrt{d_{com}} - \sqrt{d_{alloy}}) \quad (5)$$

where K is Hall-Petch coefficient ~0.13 MPa $m^{1/2}$ (34), d_{com} and d_{alloy} are the average grain size of nanocomposite and Mg alloy. The OM images of nanocomposites in Fig. 3 revealed that the average grain size of the Mg alloy was decreased by addition of nHA, so grain refinement in nanocomposites caused an increase in yield strength.

Another strengthening mechanism for nanocomposites derived from difference in the coefficients of thermal expansion (CTE) between nHA and matrix, in that a multidirectional thermal stress was generated at the particles/matrix interface. The increments in YS due to the CTE mechanism can be calculated by Eq. (6):

$$\Delta\sigma_{CTE} = \alpha G b \sqrt{\frac{12\Delta T \Delta C f_v}{bd}} \quad (6)$$

where α is constant ~ 1.25, G is shear modulus of the Mg alloy, ΔT is difference between temperature of process and test, ΔC is difference between CTE of Mg alloy and nHA and d and f are the average diameter and volume fraction of nHA.

And finally, an increase in YS for nanocomposite samples obtained from a suitable interfacial bonding between the Mg and nHA particles, especially for MZC-1nHA and MZC-2.5nHA. This good bonding may transfer loads from the matrix to nHA particles with large load-bearing capacity and according to Eq. (7) increase the YS:

$$\Delta\sigma_{LT} = f_v \sigma_{ym} \left(\frac{1}{2d} - 1\right) \quad (7)$$

Which its parameters were described above.

The above equations show that the YS of metal matrix composite can be modified by changing the percentage of reinforcement. Eq. (7) show that the load transfer was increased linearly by f_v and becomes more and more important mechanism in high percentages of reinforcement. So, for synthesized nanocomposite with low percentages of nHA, $\Delta\sigma_{LT}$ is low and the other strengthening mechanism like Orowan and CTE (29) could be important. The Orowan strengthening is not significant mechanism in the micro sized particulate-reinforced metal matrix composites, because the reinforcement particles are coarse and mostly lie on the grain boundaries of the matrix, it is unclear whether the Orowan mechanism can operate at all under these conditions. But, due to the presence of highly-dispersed nanosized reinforcement particles (smaller than 100 nm) in a metal matrix, Orowan strengthening becomes more favorable in nanocomposits, even for only a small volume fraction (<1%)(35). In nanocomposites, increase of interfacial area between the reinforcement and matrix increased the effect of CTE mechanism.

Thermal stresses around the nanoparticles large enough to cause plastic deformation in the matrix, especially in the interface region, while specimens cooled from the processing temperature. These thermal stresses was reduced quickly with increasing distance from the boundary by generating small defects such as dislocations in the close vicinity of nanosized particles (36).

The experimental results indicated that the YS of nanocomposites was increased by addition of nHA up to 2.5 %wt. and after that was decreased for MZC-5nHA. Some agglomerations and large clusters of nHA in MZC-5nHA which was shown in Fig. 5 may decreased its strength in comparison with that of MZC-2.5 nHA. Zheng et al. (37) also reported that the agglomeration of HA at high percentages caused a decrease in strength and ductility of Mg/ HA composite.

4. CONCLUSION

This work described the preparation processes for nanocomposite of Mg-5Zn-0.3Ca/ nHA by powder metallurgy and investigated the microstructures and compressive strength of nanocomposites with different amounts of nHA. The results revealed that the homogenous

nanocomposite which was prepared by this process at low percentages of nHA and at presence of nHA in nanocomposites did not prevent eutectic transformations at sintering process. The results also indicated that addition of nHA as reinforcement caused a reduction in average grain size and an increment in density of Mg alloy. Compressive strength of nanocomposites was improved due to the presence of nanoparticles by four strengthening mechanisms. However, high percentages of nHA were agglomerated in grain boundaries and disordered properties of nanocomposites. Agglomerated nHA particles formed a lot of pores in structure of nanocomposites and reduced their density and compressive strength.

REFERENCES

1. Witte, F., Ulrich, H., Rudert, M., Willbold, E.. "Biodegradable magnesium scaffolds: Part 1: appropriate inflammatory response", Journal of biomedical materials research Part A. 2007, 81(3), 748-756.
2. Yin, P., Li, N. F., Lei, T., Liu, L., Ouyang, C., "Effects of Ca on microstructure, mechanical and corrosion properties and biocompatibility of Mg–Zn–Ca alloys", Journal of Materials Science: Materials in Medicine. 2013, 24(6), 1365-1373.
3. Wang, X., Li, J., Xie, M., Qu, L, Zhang, P., Li, X., "Structure, mechanical property and corrosion behaviors of (HA+ β-TCP)/Mg–5Sn composite with interpenetrating networks", Materials Science and Engineering: C. 2015, 56, 386-392.
4. Staiger, M.P., Pietak, A. M., Huadmai, J., Dias, G., "Magnesium and its alloys as orthopedic biomaterials: a review. Biomaterials. 2006, 27(9), 1728-1734.
5. Salahshoor, M., Guo, Y., "Biodegradable orthopedic magnesium-calcium (MgCa) alloys, processing, and corrosion performance. Materials", 2012, 5(1), 135-155.
6. Yang, J., Lu, X., Blawert, C., Di, S., Zheludkevich, M. L., "Microstructure and corrosion behavior of Ca/P coatings prepared on magnesium by plasma electrolytic oxidation. Surface and Coatings Technology. 2017, 319, 359-369.
7. Zhang, B., Wang, Y., Geng, L., "Research on Mg-Zn-Ca alloy as degradable biomaterial. Biomaterials-Physics and Chemistry" InTech, 2011.
8. Du, H., Wei, Z., Liu, X., Zhang, E., "Effects of Zn on the microstructure, mechanical property and bio-corrosion property of Mg–3Ca alloys for biomedical application", Materials Chemistry and Physics, 2011, 125(3), 568-575.
9. Xu, Z, Smith, C., Chen, S., Sankar, J.. "Development and microstructural characterizations of Mg–Zn–Ca alloys for biomedical applications", Materials Science and Engineering: B, 2011, 176(20), 1660-1665.
10. Xiong, G., Nie, Y., Ji, D., Li, J., Li, C., Li, W., "Characterization of biomedical hydroxyapatite /magnesium composites prepared by powder metallurgy assisted with microwave sintering. Current Applied Physics", 2016, 16(8), 830-836.
11. Khalil, K. A., "A new-developed nanostructured Mg/HAp nanocomposite by high frequency induction heat sintering process", IOP Conference Series: Materials Science and Engineering; 2012, IOP Publishing.
12. Mahdy, A. A., "Fabrication and Characterizations of Mg/SiC Composite Via Compo-Casting Technique, Journal of American Science. 2014, 10(10).
13. D. Ahmadkhaniha, M. F., Heydarzadeh Sohi, M., Zarei Hanzaki, A., Deflorian, F., "Corrosion behavior of magnesium and magnesium–hydroxyapatite composite fabricated by friction stir processing in Dulbecco's phosphate buffered saline", Corrosion Science. 2016, 104, 319–329.
14. Li, J., Huang, Y., "Microstructure and mechanical properties of an Mg-3Zn-o. 5Zr-5HA nanocomposite processed by ECAE". IOP Conference Series: Materials Science and Engineering, 2014, IOP Publishing.
15. Lim, P., Lam, R., Zheng, Y., Thian, E.. "Magnesium-calcium/hydroxyapatite (Mg-Ca/HA) composites with enhanced bone differentiation properties for orthopedic applications. Materials Letters. 2016, 172, 193-197.
16. Zheng, Y., XG, Xi, Y., Chai, D., "In vitro

degradation and cytotoxicity of Mg/Ca composites produced by powder metallurgy. Acta Biomaterialia, 2010, 6, 1783–1791.
17. Aboudzadeh, N., Imani, M., Shokrgozar, M. A., Khavandi, A., Javadpour, J., Shafieyan, Y., "Fabrication and characterization of poly (D, L-lactide-co-glycolide)/hydroxyapatite nanocomposite scaffolds for bone tissue regeneration. Journal of Biomedical Materials Research Part A, 2010, 94(1),137-145.
18. Standard, A., "E9-09. Standard test method for compression testing of metallic materials at room temperature Philadelphia", USA: ASTM International, 2002.
19. Khanra, A. K., Jung, H. C., Yu, S. H., Hong, K. S., Shin, K. S., "Microstructure and mechanical properties of Mg-HAP composites". Bulletin of Materials Science, 2010, 33(1), 43-47.
20. D. Ahmadkhaniha M. F., Heydarzadeh Sohi, M., Zarei Hanzaki, A., Deflorian, F., "Corrosion behavior of magnesium and magnesium–hydroxyapatitecomposite fabricated by friction stir processing in Dulbecco'sphosphate buffered saline", Corrosion Science. 2016, 104, 319–329.
21. Levi, G., Avraham, S., Zilberov, A., Bamberger, M., "Solidification, solution treatment and age hardening of a Mg–1.6 wt.% Ca–3.2 wt.% Zn alloy", Acta Materialia, 2006, 54(2), 523-530.
22. Witte, F., Feyerabend, F., Maier, P., Fischer, J., Störmer, M., Blawert, C., "Biodegradable magnesium–hydroxyapatite metal matrix composites", Biomaterials. 2007, 28(13), 2163-2174.
23. Razavi, M., Fathi, M., Meratian, M., "Fabrication and characterization of magnesium–fluorapatite nanocomposite for biomedical applications. Materials characterization", 2010, 61(12),1363-1370.
24. Liu, D. B., Chen, M. F., Ye, X. Y., "Fabrication and corrosion behavior of HA/Mg-Zn biocomposites", Frontiers of Materials Science in China. 2010, 4(2), 139-144.
25. Muralithran, G., Ramesh, S., "The effects of sintering temperature on the properties of hydroxyapatite". Ceramics International. 2000, 26(2), 221-30.
26. Salleh, E. M., Zuhailawati, H., Ramakrishnan, S., Dhindaw, B. K., "Enhanced Mechanical Properties and Corrosion Behavior of Biodegradable Mg-Zn/HA Composite", Metallurgical and Materials Transactions A. 2017, 48(5), 2519-2528.
27. Feng, A., Han, Y., "Mechanical and in vitro degradation behavior of ultrafine calcium polyphosphate reinforced magnesium-alloy composites". Materials & Design. 2011, 32(5), 2813-2820.
28. Hornberger, H., Virtanen, S., Boccaccini, A., "Biomedical coatings on magnesium alloys–a review". Acta biomaterialia. 2012, 8(7), 2442-2455.
29. Yuan, Q., Zeng, X., Wang, Y., Luo, L., Ding, Y., Li, D., "Microstructure and mechanical properties of Mg-4.0 Zn alloy reinforced by NiO-coated CNTs". Journal of Materials Science & Technology, 2017, 33(5), 452-460.
30. Yan, Y., Kang, Y., Li, D., Yu, K., Xiao, T., Deng, Y., "Improvement of the mechanical properties and corrosion resistance of biodegradable β-Ca 3 (PO 4) 2/Mg-Zn composites prepared by powder metallurgy: The adding β-Ca 3 (PO 4) 2, hot extrusion and aging treatment", Materials Science and Engineering: C. 2017.
31. Li, W. J., Deng, K. K., Zhang, X., Wang, C. J., Kang, J. W., Nie, K. B., "Microstructures, tensile properties and work hardening behavior of SiCp/Mg-Zn-Ca composites", Journal of Alloys and Compounds. 2017, 695, 2215-2223.
32. Li, W. J., Deng, K. K., Zhang, X., Nie, K. B., Xu, F. J., "Effect of ultra-slow extrusion speed on the microstructure and mechanical properties of Mg-4Zn-0.5 Ca alloy", Materials Science and Engineering: A. 2016, 677, 367-375.
33. Nguyen, Q., Gupta, M., "Enhancing compressive response of AZ31B magnesium alloy using alumina nanoparticulates. Composites Science and Technology", 2008, 68(10), 2185-2192.
34. Deng, K., Shi, J., Wang, C., Wang, X., Wu, Y., Nie, K., "Microstructure and strengthening mechanism of bimodal size particle reinforced magnesium matrix composite", Composites Part A: Applied Science and Manufacturing. 2012, 43(8), 1280-1284.
35. Zhang, Z., Chen, D., "Consideration of Orowan strengthening effect in particulate-reinforced metal matrix nanocomposites: a model for predicting their yield strength", Scripta

Materialia. 2006, 54(7), 1321-1326.
36. Choi, S. M., Awaji, H., "Nanocomposites—a new material design concept", Science and Technology of Advanced Materials. 2005, 6(1), 2-10.
37. Gu, X., Zhou, W., Zheng, Y., Dong, L., Xi, Y., Chai, D., "Microstructure, mechanical property, bio-corrosion and cytotoxicity evaluations of Mg/HA composites. Materials Science and Engineering: C, 2010, 30(6), 827-832.